Ab initio calculation and quasiclassical dynamics study of the two lowest potential energy surfaces of the O(1D)+HBr system*

ARTICLE *in* INTERNATIONAL JOURNAL OF QUANTUM CHEMISTRY · OCTOBER 2001

Impact Factor: 1.43 · DOI: 10.1002/qua.1608

Ab Initio Calculation and Quasi-Classical Dynamics Study of the Two Lowest Potential Energy Surfaces of the $O(^1D) + HBr$ System*

MARÍA LUZ HERNÁNDEZ,[1] JOSÉ MARÍA ALVARIÑO,[2] ANTONIO LAGANÀ,[3] MARZIO ROSI,[3] ANTONIO SGAMELLOTTI[3]

[1]*Departamento de Física de la Atmósfera, Universidad de Salamanca, 37008 Salamanca, Spain*
[2]*Departamento de Química Física, Universidad de Salamanca, 37008 Salamanca, Spain*
[3]*Dipartimento di Chimica, Università di Perugia, 06123 Perugia, Italy*

Received 4 October 2000; revised 19 March 2001; accepted 9 May 2001

ABSTRACT: The lowest singlet $1^1A'$ and $1^1A''$ potential energy surfaces (PES) of the $O(^1D) + HBr$ system have been ab initio computed. The complete active space self-consistent field (CASSCF) method was used in most of the calculations, considering all the valence orbitals as active. The calculations were complemented with both analytical gradient calculations to characterize the stationary points and multireference configuration interaction (MRCI) calculations at selected nuclear geometries to improve the determination of the barrier heights and of the energetics. Electronic energy values for both PESs were then independently fitted by polynomial expansions in bond order coordinates. On the fitted surfaces quasi-classical trajectories were separately run. Single-surface calculations behave qualitatively different for the ground and the excited PES at low collision energies. A satisfactory agreement with existing experimental data was obtained by using the ground PES while calculations performed on the excited $1^1A''$ PES worsened the agreement. However, when collision energy is increased, detailed experimental distributions are less well reproduced by calculations on the ground PES. This may imply the participation via nonadiabatic transitions of the $2^1A'$ PES at higher energies while the adiabatic ground singlet PES well describes reactive scattering at low collision energy. Int J Quantum Chem 86: 79–89, 2002

Key words: chemistry of the atmosphere; electronically excited reagents; molecular beam experiments; ab initio electronic structure calculations; quasiclassical nuclear dynamics

Correspondence to: J. M. Alvariño; e-mail: alva@gugu.usal.es.

*Parts of this work were presented as poster 10-TH at the COMET XVI Conference, Assisi, June 20-25, 1999.

Contract grant sponsor: DGICYT of Spain.
Contract grant number: PB98-0281.
Contract grant sponsors: MURST; CNR; and ASI of Italy; Action D9 of the COST in Chemistry.

Introduction

Reactions of electronically excited reagents are of importance in stratospheric chemistry. There, molecular species (including ozone) easily dissociate under the action of solar ultraviolet (UV) radiation [1]. Particularly active as reagents are the metastable species produced in the photolysis processes since, because of their intrinsic long lifetime, they have a greater chance of using the excess energy in a variety of chemical processes. Due to the atmospheric abundance of O- and N-containing molecules, atomic oxygen singlet, $O(^1D)$ (lifetime $\approx$150 s), and atomic nitrogen doublet, $N(^2D)$ (lifetime $\approx$26 h), are exceedingly important metastable reagents. Their elementary chemistry has been recently reviewed [2].

At the same time, bromine is believed to be responsible of much of the ozone loss despite its much lower stratospheric concentration with respect to chlorine. Bromine is, in fact, present in an "active" form (species that directly react with ozone as opposite to "reservoir" species, which, as is the case of chlorine, are rather stable). In this article, we refer to the $O(^1D)+HBr$ reaction as a prototype for reactions of $O(^1D)$ with brominated compounds.

The electronic excitation of $O(^1D)$ (45.4 kcal mol^{-1} over the ground state, $O(^3P)$) makes both product chemical channels open at thermal energies. It is, in fact, $\Delta H_0^0 = -60.5$ kcal mol^{-1} for reaction

$$O(^1D) + HBr(^1\Sigma^+) \rightarrow OH(^2\Pi) + Br(^2P) \quad (1)$$

and $\Delta H_0^0 = -14.0$ kcal mol^{-1} for reaction

$$O(^1D) + HBr(^1\Sigma^+) \rightarrow BrO(^2\Pi) + H(^2S). \quad (2)$$

The fivefold electronic degeneracy of $O(^1D)$ is split upon approach of $HBr(^1\Sigma^+)$ and three singlet adiabatic potential energy surfaces (of symmetry Σ^+, Π, and Δ in $C_{\infty v}$) arise. Of these only the $^1\Pi$ surface asymptotically connects reagents to both $OH(^2\Pi)$ + $Br(^2P)$ and $BrO(^2\Pi)$ + $H(^2S)$. This is also the only adiabatic surface derived from the latter products. Meanwhile four potential energy surfaces (PES) (of symmetry Σ^+, Π, Δ, and Σ^- in $C_{\infty v}$) stem from $OH(^2\Pi)$ + $Br(^2P)$. PES doubly degenerate in $C_{\infty v}$ further split into A' and A'' surfaces in C_s while Σ^+ and $\Sigma^- C_{\infty v}$ species correlate with A' and A'', respectively, in C_s. Stable isomers HOBr and HBrO are intermediates in the dynamics of reactions under study, and their ground state is $1^1A'$ ($^1\Sigma^+$ in $C_{\infty v}$). The whole electronic structure subject bears resemblance to that for the much studied $O(^1D)+H_2(^1\Sigma_g^+)$ reaction (see Ref. [3]) and, especially, for $O(^1D)$ + $HCl(^1\Sigma^+)$ (see Ref. [4]). In this work we shall refer just to the electronically ground $1^1A'$ and first excited $1^1A''$ surfaces for $O(^1D) + HBr(^1\Sigma^+)$.

The experiment more directly related to our calculations is the beam experiment of Balucani et al. [5], although of direct relevance is also the more recent kinetic experiment of Cronkhite and Wine [6]. The interested reader should consult these two articles for reference to all the other (kinetic) experiments. Ab initio calculations on the electronic structure of intermediate triatomic molecules (the well regions of the ground potential energy surface) have been performed by Lee [7] and, more recently, results of a coupled-cluster calculation have been published by Li and Francisco [8]. Also Fusti-Molnar et al. [9] have published results of a theoretical investigation of the potential energy surface of the title system. Their interest focused on the ground and two first excited potential energy surfaces [9] for the study of the dynamics of the photodissociation process $HOBr + h\nu \rightarrow OH + Br$. These results cannot be directly related to experimental reactive studies like those in Ref. [5] since, during the calculations, the OH internuclear distance was kept constant at its equilibrium value while a strong vibrational inversion of OH is a fingerprint of the OH + Br channel (see Ref. [5]). Our calculations were instead extended to all the configuration regions relevant to reactions (1) and (2), and this is the first attempt to simulate the beam experiment [5] by means of dynamical calculations performed on ab initio potential energy surfaces.*

The work is organized as follows. In the following section, details about the method adopted for the calculation of the electronic energy given, and the main features of the calculated potential energy values are compared with spectroscopic data and other published theoretical information. Then, the shape of the fitted potential energy surfaces (PESs) is illustrated and details of the quasi-classical trajectories (QCT) calculations are given. Results of the dynamical investigation are reported in the fourth section and compared with available experimental data. Our conclusions are given in the final section.

*When all our ab initio, fit, and dynamical calculations were completed and the manuscript essentially ready, a new, global ab initio (MRCI) $1^1A'$ surface was announced [Peterson, K. A. J Chem Phys 2000, 113, 4598–4612]. No dynamical tests have so far been undertaken on this PES to see how it works in a comparison with the beam experiment.

TABLE I
Diatomic equilibrium bond lengths (in Å) and binding energies (in eV).

Method	CASSCF		MRCI		MRCI + Q		Exp.[a]	
	r_e	D_e	r_e	D_e	r_e	D_e	r_e	D_e
OH	0.978	3.563	0.964	4.151	0.964	4.204	0.970	4.621
HBr	1.425	3.281	1.404	3.621	1.403	3.642	1.414	3.921
BrO	1.839	1.018	1.790	1.703	1.791	1.896	1.717	2.438

[a] Data taken from Ref. [14].

Ab initio Calculations

Ab initio calculations have been performed following the same general strategy adopted for the similar O(^1D)+HCl system [10]. The complete active space self-consisted field (CASSCF) method was used in most of the study. All the valence orbitals were considered as active. This means that there are 14 active electrons in 9 active orbitals. Analytical gradient calculations using the CASSCF wave function were performed to localize the stationary points on both surfaces. Multireference configuration interaction (MRCI) calculations were subsequently performed at selected nuclear geometries to improve the determination of the barrier heights and the energy balance. Since the use of all the CASSCF configurations as references in the MRCI calculations leads to prohibitively long CI expansions, a selection of references was performed. All the valence electrons were correlated and a direct method was used for CI calculations [11]. Davidson's correction [12] was also included to account for the effect of higher excitations. We shall refer to this level of calculation as MRCI + Q. All computations were performed using the GAMESS-UK [13] program package, implemented on a cluster of IBM RS6000 workstations.

Table I shows the diatomic bond distance values computed at various levels of accuracy. For comparison also experimental values are given. The table evidences that in our calculations the description of the Br–O bond is somewhat less accurate than that of O–H and H–Br bondings.

Table II shows the ergicity and the barrier height at various levels of approximation for the two collinear reaction channels in the $^1\Pi$ surface. It can be immediately seen that, while the OH+Br forming reaction is definitely exoergic at all levels of calculations, the reaction leading to BrO + H is computed to be endoergic at the CASSCF level. However it becomes exoergic also at the CASSCF level with the inclusion of zero-point energy. At MRCI and MRCI + Q levels, the reaction is calculated to be definitely exoergic.

At the MRCI + Q level, the collinear O–H–Br potential has a small barrier of 1.4 kcal/mol at $r_{OH} = 1.627$ Å and $r_{HBr} = 1.429$ Å, while the collinear O–Br–H potential has a higher barrier of 10.1 kcal/mol at $r_{BrO} = 2.009$ Å and $r_{HBr} = 1.600$ Å. As apparent from Table II that the height of the collinear barriers is largely overestimated when using lower level approaches. This confirms the importance of introducing dynamical correlation effects when evaluating the energetics of the reactive processes. On the contrary, as is well known, the molecular geometry

TABLE II
Exoergicity and collinear barrier height (in kcal/mol; over reagents) on the $^1\Pi$ surface.[a]

Method	O(^1D) + HBr → OH + Br		O(^1D) + HBr → H + BrO	
	Barrier height	Energy balance	Barrier height	Energy balance
CASSCF	7.1 (6.9)	−47.5 (−46.1)	26.7 (24.0)	0.7 (−1.8)
MRCI	3.2 (3.0)	−61.1 (−59.5)	18.4 (15.7)	−4.4 (−6.9)
MRCI + Q	1.6 (1.4)	−62.5 (−60.9)	12.9 (10.1)	−10.4 (−12.9)

[a] In brackets, values corrected for the zero-point energy.

TABLE III

CASSCF geometry (in Å and degrees) and energy (in kcal/mol from the lowest HOBr minimum and without zero-point energy correction) of stationary points on the $^1A'$ surface compared to our fit, and other calculated and experimental data.[a]

	Minimum HOBr	Minimum HBrO	Saddle[b]
r_{OH}	0.977 (0.970) {0.964} [0.961]	2.646 (2.386) {2.527} [2.554]	1.967 (1.805) {1.724}
r_{BrO}	1.903 (1.849) {1.841} [1.834]	1.804 (1.800) {1.710} [1.731]	2.033 (1.794) {1.879}
∠(HOBr)	101.9 (107.5) {102.9} [102.3]	31.7 (40.2) {33.7} [33.3]	41.9 (54.2) {47.2}
E	0	79.4 (68.8) {58.9} [61.5]	92.4 (75.1) {78.6}

[a] In parentheses fitted values; in curly brackets calculated values from Ref. [8]; in square brackets experimental values from Ref. [15].
[b] Between minima, i.e., isomerization saddle point.

is much less sensitive to the introduction of dynamical correlations.

Moving out of collinearity, the $^1\Pi$ surface splits into the two surfaces $1^1A'$ and $1^1A''$. Using gradient techniques at the CASSCF level we have localized on the $1^1A'$ surface the stationary points reported in Table III. The first two stationary points are minima corresponding to the stable isomers HOBr and HBrO. The third stationary point is the isomerization saddle connecting the HOBr and HBrO minima. The geometry of HOBr, evaluated at the CASSCF level, is in reasonable agreement with the experimental structure and with the more accurate ab initio calculations of Refs. [7–9]. The deviation of the r_{BrO} value is due to the difficulty of describing at ab initio level the BrO bond. The agreement with previous multiconfiguration SCF (MCSCF) calculations [16] is, as expected, excellent. The geometry of HBrO, evaluated at the CASSCF level, is also in reasonable agreement with the calculations of Lee [7] and Li and Francisco [8]. The main deviation occurs for the r_{BrO} bond and its value confirms that correlation effects are not so crucial in determining the geometry of equilibrium structures. The relative stability of HOBr and HBrO is overestimated with respect to the value reported in Ref. [8] even when using an MRCI + Q approach, implying that to achieve chemical accuracy a higher level of correlation needs to be introduced.

The $1^1A''$ PES was also computed at the CASSCF level. The ab initio surface appears very flat and mainly dissociative in nature.

Fitted Potential Energy Surfaces

To fit the ab initio values a functional form of the many body (MB) bond order (BO) type [17] was used. First of all, ab initio points were modified by scaling them to the MRCI + Q ones and, thereafter, to account for differences at the asymptotes between exoergicities calculated with the modified points and experimental values. The procedure follows our usual method (see, e.g., [10, 18]). Particular care was taken in damping the electronic excitation of O(^1D) while proceeding from the O(^1D) + HBr asymptote to the close interaction region. This is needed to ensure a common dissociation limit for the three diatomic molecules. As in the case of the closely related O(^1D) + HCl system [18], we altered the long-range part of the hydrogen halide diatomic term of the MB functional using hyperbolic tangent functions in the internuclear distance of the diatomic reagent. More precisely, the following form was adopted:

$$V_{2,\mathrm{HBr}} = V^0_{2,\mathrm{HBr}} \tanh(+) + E^*\{1 - \tanh(-)\}, \quad (3)$$

where $V^0_{2,\mathrm{HBr}}$ is the unmodified HBr diatomic potential, E^* is the electronic excitation energy of O(^1D), $\tanh(\pm) = 0.5\{1-\tanh(\pm y)\}$, and $y = a(r_{\mathrm{HBr}} - br_{e,\mathrm{HBr}})$. Here a and b have been optimized to the values $a = 6.25$ Å^{-1} and dimensionless unit $b = 1.5$. This correction does not affect the diatomic force constants and the turning-point locations of the lowest vibrational levels. It only affects the long-range tail of the reactant diatomic potential so that only vibrational energy levels of HBr higher than $v = 7$ start deviating from the exact value. In any event, our dynamical calculations are performed at much lower vibrational energy and, therefore, do not explore this region of the PES.

For the remainder, the fitting procedure is the same as the one used in Ref. [10]. It makes use of an MBBO polynomial. In this formulation the potential V is expressed as $V = V_2 + V_3$ with V_3 being the three-body term and V_2 being the sum of the three

two-body ones, $V_{2,i}$. The form of the single two-body polynomial is $V_{2,i} = -D_{e,i} \sum_j a_{j,i} n_i^j$ for product diatoms and for $V^0_{2,\mathrm{HBr}}$ but $V_{2,\mathrm{HBr}}$ is modified to account for the electronic excitation of O(^1D) in the way described above. The bond order variable is $n_i = \exp[-b_i(r_i - r_{e,i})]$ [17], with r_i being the internuclear distance ($r_{e,i}$ is the related equilibrium value), and b_i and $a_{j,i}$ are the fitting parameters whose values are determined by optimizing the reproduction of the force constants of the related diatom [17]. The polynomial of the two-body terms is of the fourth order (j = 1–4). The form of the three-body polynomial is $V_3 = \sum_{jkl} c_{jkl} n_1^j n_2^k n_3^l$, where c_{jkl} are the three-body fitting coefficients and $j + k + l$ never exceeds 6.

On the other hand, the excited PES—there being neither experimental non theoretical calculations for excited states of the intermediate triatomics to compare and eventually correct—retains the form $V = V_2 + V_3$, where only the coefficients of the three-body term are at variance with respect to the ground PES. Our two PES are completely independent from each other; in other words, the excited surface is completely uncoupled from the ground one, i.e., nonadiabatic transitions are absent from our scheme. Our QCT calculations, therefore, resemble those of Schatz et al. [19] and Aoiz et al. [20] on the related O(^1D) + H_2, D_2, HD reactions.

Stationary points in the fitted PES have been located using POLYRATE [21]. Results are collected in Tables III–VI. Geometry and energy values are in reasonable agreement with published values from other origin (see Table III). Taking into account the difficulty of fitting a surface with two product channels and two deep wells and the saddle between them, the same can be said for the harmonic frequencies (Tables IV–VI) with the exception of the OH and HBr stretching frequencies in HOBr and HBrO, respectively. Therefore, to see whether a surface modified to better fit the harmonic field of the intermediate triatomics would be a better representation for the dynamics we added to our PES three-dimensional Gaussians centered at the HOBr and HBrO minima and with appropriate curvatures (as given by the coefficients of the three exponentials taken from [7]). However, while distributions on the modified surface did not appreciably change with respect to the original PES, the Gaussian artifact had the effect of producing an erratic dependence of the cross sections with collision energy instead of the monotonic decrease expected for exoergic, barrierless reactions [24] and actually obtained on the fitted PES. To summarize, it appears that a reproduction of the harmonic (normal mode) frequency values of the very bottom of the PES is not critical to the quasi-classical dynamics evolving at energies at least 120 kcal/mol above.

Although an analytical representation of the potential energy surface (and its derivatives) is, of course, necessary for a realistic dynamical calculation, a graphical representation is very convenient to help rationalize observed behaviors, approximately localizing stationary points on the surface, etc. In the first stages of fitting single energy points from an ab initio calculation a graphical study of the obtained PES can help detect spurious features with eventual catastrophic consequences for the dy-

TABLE IV
Calculated and experimental vibrational harmonic frequencies (in cm^{-1}) of HOBr on the $^1A'$ surface.

	This work	LF[a]	Exp.[b]
ν_1(*s*, HO)	5324	3833	3610
ν_2(*b*)	1333	1174	1163
ν_3(*s*, BrO)	898	621	620

[a] Ref. [8].
[b] Ref. [22].

TABLE V
Calculated and experimental vibrational harmonic frequencies (in cm^{-1}) of HBrO on the $^1A'$ surface.

	This work	LF[a]	Exp.[b]
ν_1(*s*, HBr)	2852	2360	2333
ν_2(*b*)	847	837	—
ν_3(*s*, BrO)	731	705	668

[a] Ref. [8].
[b] Ref. [23].

TABLE VI
Calculated vibrational harmonic frequencies (in cm^{-1}) of the isomerization saddle on the $^1A'$ surface.

	This work	LF[a]
ν_1	2356	2499
ν_2	709	561
ν_3	956i	1234i

[a] Ref. [8].

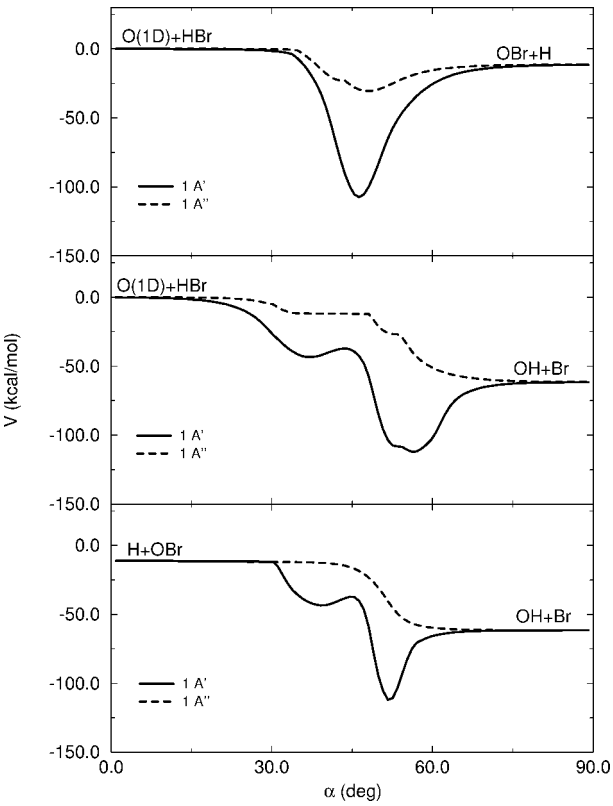

FIGURE 1. Minimum energy path on the $1A'$ (solid line) and $1A''$ (dashed line) potential energy surfaces for the BrO + H channel (top panel), for the OH + Br channel (middle panel) and for the interconversion between both of them (bottom panel) featuring the isomerization reaction and its saddle.

namics. Only diatomic molecules can have their potential energy surfaces (curve, in this case) plotted in a single graph, a planar plot of energy vs. internuclear distance, the one and only geometrical variable for two nuclei. In a triatomic system, since we have three geometric variables, a graphical representation of the whole potential energy surface in a single plot is not feasible. One is therefore forced to make physically sound "cuts" through the PES keeping constant at least one geometrical parameter. Sketches of this kind of some important features of the fitted ground and excited PESs are given in Figures 1 and 2.

Figure 1 shows the minimum energy path (MEP) for both the less exoergic (BrO + H) and the more exoergic (OH + Br) channel as well as for the BrO + H → OH + Br reaction. In this plot, the abscissa α (a sort of "reaction coordinate") is an angle ranging from 0° (for reagents) to 90° (for products) and it is calculated as follows. For reaction (1), say, and a given value of the internal $\theta_H = \widehat{OHBr}$ angle, a turning center in the $(r_{OH} - r_{HBr})$ plane is placed with the coordinates (in Å) (10,10) (i.e., far away from the strong interaction zone), and from there perpendicular lines are drawn to the r_{OH} axis (thus defining the reagents configuration as $\alpha = 0$) and the r_{HBr} axis (what defines the products configuration OH + Br as $\alpha = 90°$). Lines at other α angle values within the range (0°, 90°) correspond to intermediate configurations between reagents and products. The minimum energy value along any such α-line is sought for and the mimimum of minima (as the θ_H angle is scanned) is a point on the MEP for the particular value of α being considered. The locus of minima is the MEP for reaction (1) and the same with opportune changes applies for reaction (2) and for the BrO+H → OH+Br reaction. Notice that this is an operational MEP using an ad hoc definition of reaction coordinate instead of the "intrinsic reaction coordinate" [25] of use in variational transition-state theory and multidimensional semiclassical tunneling calculations [26] and calculated by POLYRATE.*

Although small barriers are seen in collinear configurations,† inspection of Figure 1 lets see no noticeable barrier on any of the MEPs. This absence of barrier for noncollinear configurations is specially remarkable as regards the excited surface. In fact, the related $O(^1D)+H_2$, D_2, HD reactions [19, 20] display an entrance saddle (albeit small) for the $1^1A''$ surface. For the remaining, the MEP on the excited surface (shown as dashed lines on Fig. 1) of our system shows an intermediate region of energy below that of asymptotes for the BrO + H channel (but we found no true minimum), while the way toward OH+Br and the path linking both product channels are less structured.

Now we consider the more important MEP for the ground PES. The lower ($1^1A'$) path leading to OH + Br (solid line in the middle panel of Fig. 1) distinctly passes through both the deeper ("insertion" or "HOBr" well according to the definition of Ref. [28]) and the shallower ("abstraction" or

*Due to the absence of a genuine transition state for reactions (1) and (2), the standard MEP calculation in [21] starts at the isomerization saddle and does not stretch beyond the HOBr minimum, on the one side, and the HBrO minimum, on the other side, i.e., it does not cover the whole configuration space of our reactions as plotted on Figure 1.

†These collinear barriers on the ground PES are (the cusps of) the conical intersections between low-lying Σ^+ and Π singlet states (see, e.g., Ref. [27]). As the triatom bends over and the $1^1A'$ and $1^1A''$ (and $2^1A'$) surfaces merge, the height of the barrier decreases and it eventually disappears, i.e., it does not show up on the MEPs.

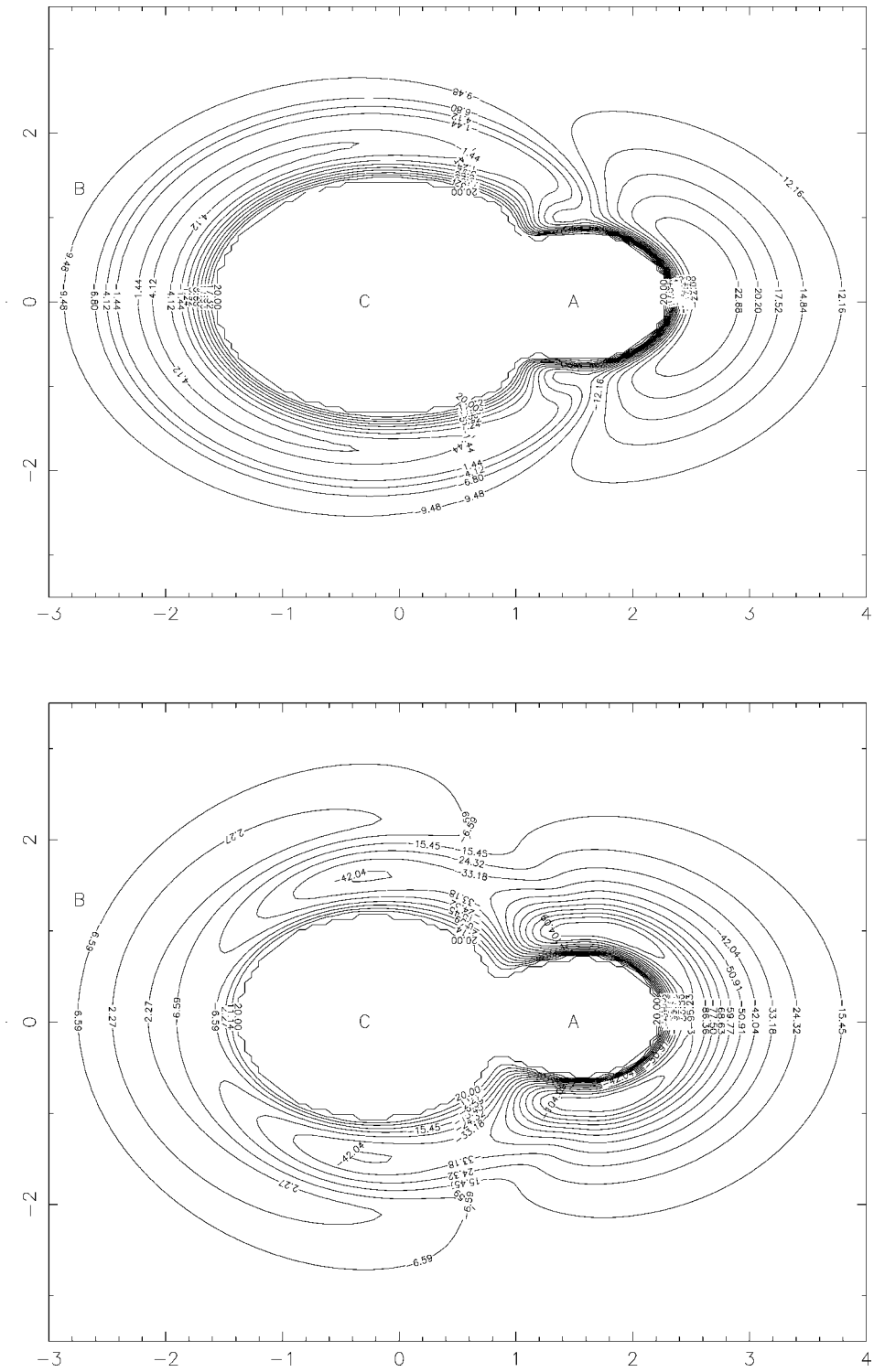

FIGURE 2. Polar plot of the ground (bottom panel) and excited (top panel) potential energy surface for the O(^1D) + HBr system. The origin of coordinates is set at the center of mass of BrO, which lies on the *X* axis with the internuclear distance varying in the range $\{1.8 \pm 0.2\}$ Å in order to minimize the potential energy value. Energies and distances are given in kcal mol^{-1} and Å, respectively. The energy zero is set at the reagents asymptote. Letters have the following meaning: A and C are the approximate (remember the relaxation allowed to the BrO distance) positions of the O and Br atoms, respectively; B indicates the wandering position of the H atom.

"HBrO" well [28]). Using POLYRATE [21] we found that energy values at minima are 112.3 (for the HOBr well) and 43.5 kcal mol^{-1} (for the HBrO well) below the reagents' asymptotic minimum. This makes HOBr 68.8 kcal mol^{-1} more stable than HBrO (see Table III).

The MEP on the ground PES leading to BrO + H (solid line in the top panel of Fig. 1) clearly passes through the HOBr well while the shallower HBrO well appears to be "obscured" or "absorbed" in our plot by parts of the attractive branches of the deepest well actually deeper than even the bottom of the HBrO well. Finally, the bottom panel represents the MEP for the interconversion between both reaction products BrO+H and OH+Br. This plot very neatly shows the minimum energy profile for the isomerization reaction and the saddle between HOBr and HBrO. It is appealing to see the plot as the minimum energy path for proton migration from HBrO to HOBr structures [29].

Another graphical representation of the potential energy surface of a triatomic system that is very instructive for systems featuring one or more stable intermediate complexes is the one shown in Figure 2 [18, 30]. In these plots a diatomic molecule (generally, but not in this case, the reactant molecule is chosen) is placed with its internuclear axis on the X axis and its center of mass sitting at the origin of the coordinate system. The isolated atom is then allowed to move around the molecule on the XY plane. The potential energy is calculated for each of these triatomic configurations to draw equipotential contours. In doing so, the internuclear diatomic distance can be either kept constant (e.g., at the equilibrium value) or varied by minimizing (within certain limits) the value of the potential energy to give a dynamics-oriented picture of the potential. In our case, we chose BrO as the diatomic molecule because the equilibrium BrO internuclear distance for both stable isomers in the ground PES (see Table III) is close to 1.8 Å. By allowing it to vary in the range $\{1.8 \pm 0.2\}$ Å we can describe both minima by using a single plot. The plot is, of course, symmetrical around the X axis. This graph can be seen as describing the large amplitude motion of H around the BrO core in the HOBr molecule [29].

The map of the $1^1A'$ PES (bottom panel of Fig. 2) shows the two mentioned minima of the ground surface (inside the contours at about -42 kcal mol^{-1} for the HBrO well and -104 kcal mol^{-1} for the HOBr well). It is seen, for example, that, on the ground surface, collinear attacks of H onto the Br end of BrO (coming from the left along the X axis) would face a small barrier, slightly over 2 kcal mol^{-1}, while collinear attacks of H onto the O end of BrO (coming from the right along the X axis) are attractive. On the other hand, the collinear interaction in the excited PES (see top panel of Fig. 2) is attractive (albeit moderately) on both ends of the target molecule.

Dynamical Results and Discussion

As already advanced and implied by the nature of the ab initio calculations quasiclassical trajectories were run on both PESs in a completely independent way. The usual controls of energy and angular momentum conservation [18] were performed to optimize the time stepsize and initial and final distances. Adopted values were 5×10^{-17} s and 9 Å, respectively. Other input parameters of the QCT calculation were 3.4–3.7 Å (maximum impact parameter range for the $1^1A'$ PES), 3.0–3.3 Å (maximum impact parameter range for the $1^1A''$ PES), and random selection of the initial geometry. Batches of 100,000 trajectories were then run for any set of reagents' energy (given by collision energy, E_{coll}, vibrational, v, and rotational, j, HBr quantum numbers).

A summary of total cross sections and branching ratio values for the two surfaces and collision energies is given in Table VII and compared with available experimental data [5, 6]. Exoergic reactions are very often barrierless. In other words, they feature a PES without a "genuine" (electronic) transition state, i.e., without a saddle point higher in energy than both reagents and products. As it happens in diatomic molecules with the contribution from the rotational energy and the concomitant j-dependent effective potential energy curve (determining a centrifugal barrier for the dissociation and for the reverse recombination reaction) also in polyatomic reactions a centrifugal barrier arises as the joint effect of the bare (barrierless) PES and the total angular momentum. This is a well-known fact (see, e.g., [24]) but, in addition to this, a system like ours, including as triatomic intermediates a pair of isomers, presents a more uncommon transition state (TS), the one for the isomerization reaction. This would be (it actually *is*) the normal TS for the bare isomerization reaction but, being lower in energy than some of the asymptotic channels (O(^1D) + HBr and H + BrO), it is not *the* transition state for the collision reaction. For example, the system is never just above this TS in energy but has a lot more energy (at least 45 kcal/mol in our simulations). Also,

TABLE VII

Calculated cross sections and branching ratios on the ground and ground + first excited potential energy surfaces for O(^1D) + HBr ($v = j = 0$) → BrO + H, OH + Br.

	$1A'$ E_{coll} (kcal mol^{-1})		$1A' + 1A''$ E_{coll} (kcal mol^{-1})	
	5	14	5	14
σ_{BrO} (Å^2)	7.68 ± 0.08	2.39 ± 0.04	21.6	12.5
σ_{OH} (Å^2)	21.9 ± 0.1	13.1 ± 0.1	21.9	13.4
$\Gamma = \sigma_{BrO}/\sigma_{OH}$[a]	0.35 ± 0.01	0.18 ± 0.01	0.99	0.93

[a] Experimental values: $\Gamma \geq 0.16 \pm 0.07$ at $E_{coll} = 14$ kcal mol^{-1} from Ref. [5]; $\Gamma > 0.20 \pm 0.04$ under thermalized conditions (room temperature) from Ref. [6].

no quantum tunneling can take place across it for reactions with O(^1D) + HBr as reagents.

As expected for barrierless reactions, thus, the reactive cross section on the ground surface decreases with collision energy for both chemical channels. The same qualitative result was obtained for the O(^1D) + HCl reactions in our QCT calculations [18] as well as in quantum wavepacket calculations by Bittererová et al. [31]. Previously, also Schatz and co-workers obtained quasiclassical cross sections decreasing with collision energy for the O(^1D) + H_2 ground-state reaction [19]. However, experiments for the O(^1D) + HBr reaction [5] do not provide the absolute values of the cross sections and only an experimental estimate was given for the branching ratio, $\Gamma = \sigma_{BrO}/\sigma_{OH}$. Our value ($\Gamma = 0.18 \pm 0.01$) at $E_{coll} = 14$ kcal mol^{-1} on the ground PES is in accord with the experimental value ($\Gamma \geq 0.16 \pm 0.07$) of Balucani et al. [5] obtained at the same collision energy. At the same time, the value ($\Gamma > 0.20 \pm 0.04$) of Ref. [6] (obtained from thermal rate coefficients measurements corresponding to a value of the average collision energy, $\langle E \rangle_{coll}$, of about 1 kcal mol^{-1}) is compatible with the calculated value, which is found to increase as collision energy decreases. On the other hand, branching ratios calculated as the sum of contributions from the ground and the excited surface (as done by Schatz and co-workers for the O(^1D) + H_2 reaction in [19]) would foresee three to five times more relative production of BrO than is actually found. This means that, if any, the contribution of the $1^1A''$ to the reaction is small. Agreement further worsens if double weight is given to the excited surface to somewhat account for the participation of the $2^1A'$ excited surface (see Ref. [19]). These are arguments in favor of the nonparticipation of the $1^1A''$ excited surface in the dynamics of reactions (1) and (2).

More stringent tests on the suitability of the PES for dynamical calculations come from the analysis of detailed distributions and their comparison with the experiment of Balucani et al. [5]. These authors report angular and recoil energy distributions of the BrO + H channel and the OH vibrational energy distribution.* Figure 3 compares experimental (solid lines) to calculated (dashed lines, calcula-

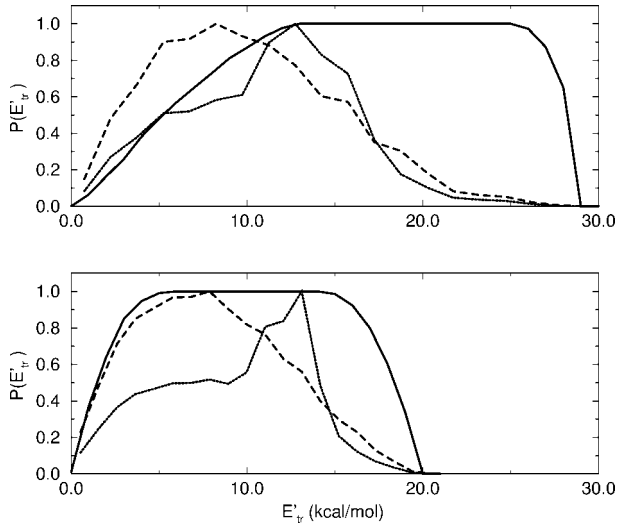

FIGURE 3. Product translational energy distribution for O(^1D) + HBr → BrO + H (dashed lines, calculations on the $1^1A'$ PES, dotted lines summed result on the $1^1A'$ and $1^1A''$ PES) calculated for $v = 0$, $j = 0$, and $E_{coll} = 5$ kcal mol^{-1} (lower panel) and $E_{coll} = 14$ kcal mol^{-1} (upper panel). For comparison data obtained from the beam experiment are also given (solid line).

*For the product angular and translational energy distributions of the BrO + H channel at $E_{coll} = 5$ kcal/mol, the average of the two model distributions of Ref. [5] was taken for comparison [32].

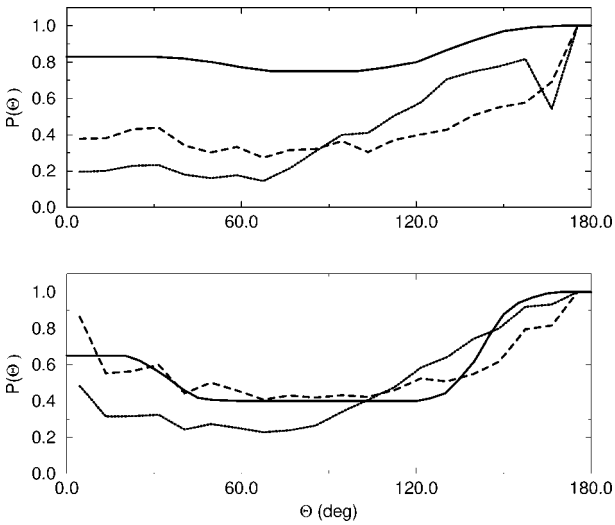

FIGURE 4. As in Figure 3 for the product angular distribution.

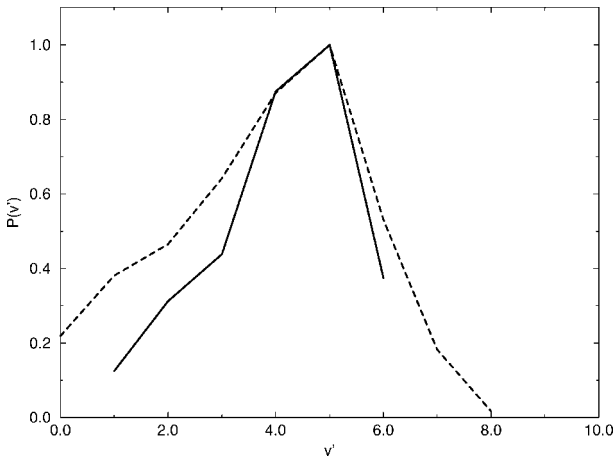

FIGURE 5. Vibrational energy distribution of OH calculated at $v = 0$, $j = 0$, and $E_{coll} = 10$ kcal mol^{-1} (dashed line). For comparison, data obtained from the FTS experiment are also given (solid line).

tions on the $1^1A'$ PES; dotted lines summed result on the $1^1A'$ and $1^1A''$ PES) product translational energy distributions for BrO + H at both 5 (top panel) and 14 kcal mol^{-1} (bottom panel) collision energy values. A reasonable agreement is obtained at $E_{coll} = 5$ kcal mol^{-1} (specially in the low recoil energy range, below 10 kcal mol^{-1}). The agreement worsens at $E_{coll} = 14$ kcal mol^{-1}. In this case the participation of the excited PES slightly helps to improve the agreement as the initial rise of the distribution concerns, but the contrary happens at $E_{coll} = 5$ kcal mol^{-1}. Summarizing, it appears that the ground surface would demand a further refinement in the BrO + H exit channel. An exit barrier, for example, could lead to an increase in the translational energy disposal [24].

A good agreement with the experiment is obtained for the BrO+H center-of-mass product angular distribution at 5 kcal mol^{-1} as shown in Figure 4 (top panel). As for other O(^1D) reactions (O(^1D) + H_2, [19]; O(^1D) + HCl, [10, 28]) rather symmetrical, backward-forward distributions with some more backward intensity are obtained. The agreement is worse at $E_{coll} = 14$ kcal mol^{-1}. And, again, little is gained if the contribution of the excited surface is taken into account.

The only property experimentally investigated for the OH+Br channel is the OH vibrational energy distribution (PVD). This was obtained by Fourier transform spectroscopy (FTS) in Ref. [5] and, according to the authors, results refer to a collision energy of 10 kcal mol^{-1}. Figure 5 shows a plot of the experimental (solid line) and theoretical (dashed line) PVDs of OH. The experimentally obtained PVD is seen to be strongly inverted with a maximum at $v' = 5$. The theoretical PVD calculated at the same energy of the experiment well mimics the shape of the experimental distribution. The only difference consists of a slight broadening of the theoretical curve with respect to the experimental one, but the overall shape of the distribution is preserved. It thus seems that the OH + Br channel is well described in our PES. Finally, although the calculated OH + Br production on the excited surface is very small (see Table VII) it appears that—while still leading to an inverted population peaking at $v' = 2$—the $1^1A''$ PES does not contribute to populate vibrational states beyond $v' = 3$, still another argument favoring the nonparticipation of the $1^1A''$ excited surface on the dynamics of this reaction. Therefore, while some degree of OH vibrational inversion appears on trajectories run on both surfaces, to achieve a large inversion depends on probing the triatomic deep double-well region [28] which, under single-surface conditions, is only achievable on the ground PES.

Conclusions

The theoretical study of the title reaction has been articulated in three steps: (1) an extended ab initio calculation of the potential energy values for the ground and first excited singlet surfaces has been carried out at the CASSCF level with selected values

improved by performing higher level calculations; (2) calculated values are independently adjusted and fitted using a many-body bond order technique; and (3) on the fitted potential energy surfaces dynamical calculations are separately performed to compare calculated quantities with experimental findings.

The comparison with measured branching ratios indicates that single PES dynamical calculations performed on the ground surface are suited for describing the reactive behavior of the system at least at not too high collision energy. This has motivated us to carry out a more detailed analysis of the reactive properties of the ground PES. For other reactive properties contributions from the excited surface, if any, have been found to play a minor role. This allows us to consider the PES obtained from our fitting a good starting point for further refinements when performing true multisurface calculations in analogy with what has been found in similar calculations reported in the literature [3, 19, 33].

ACKNOWLEDGMENTS

This work was performed with the financial support of DGICYT of Spain (grant no. PB98-0281) and of MURST, CNR, and ASI of Italy. It has been undertaken as a part of the collaborative European project of Action D9 of the COST in Chemistry initiative. We thank Simona Fantacci for her work at the initial stages of the ab initio calculation and Aurelio Rodríguez for suggestions and computational aid.

References

1. Wayne, R. P. Chemistry of Atmospheres; Clarendon Press: Oxford, 1985.
2. Casavecchia, P.; Balucani, N.; Alagia, M.; Cartechini, L.; Volpi, G. G. Acc Chem Rem 1999, 32, 503–511.
3. Schatz, G. C.; Pederson, L. A.; Kuntz, P. J. Faraday Discuss Chem Soc 1997, 108, 357–374.
4. Nanbu, S.; Iwata, S. J Phys Chem 1992, 96, 2103–2111.
5. Balucani, N.; Beneventi, L.; Casavecchia, P.; Volpi, G. G.; Kruus, E. J. Sloan, J. J. Can J Chem 1994, 72, 888–902.
6. Cronkhite, J. M.; Wine, P. H. Int J Chem Kinet 1998, 30, 555–563.
7. Lee, T. J. J Phys Chem 1995, 99, 15074–15079.
8. Li, Z.; Francisco, J. S. J Chem Phys 1999, 111, 5780–5782.
9. Fusti-Molnar, L.; Szalay, P. G.; Balint-Kurti, G. G. J Chem Phys 1999, 110, 8448–8460.
10. Hernández, M. L.; Redondo, C.; Laganà, A.; Ochoa de Aspuru, G.; Rosi, M.; Sgamellotti, A. J Chem Phys 1996, 105, 2710–2718.
11. Saunders, V. R.; Van Lenthe, J. H. Molec Phys 1983, 48, 923–935.
12. Davidson, E. R. In Daudel, R.; Pullman, B., Eds. The World of Quantum Chemistry; Reidel: Dordrecht, 1974.
13. Guest, M. F.; Sherwood, P. GAMESS-UK, User's Guide and Reference Manual; SERC Daresbury Laboratory: UK, 1992.
14. Huber, K. P.; Herzberg, G. Constants of Diatomic Molecules; Van Nostrand: New York, 1978.
15. Koga, Y.; Takeo, H.; Kondo, S.; Sugie, M.; Matsumura, C.; McRae, G. A.; Cohen, E. A. J Mol Spectrosc 1989, 138, 467–479.
16. Monks, P. S.; Stief, L. J.; Krauss, M.; Kuo, S. C.; Klemm, R. B. J Chem Phys 1994, 100, 1902–1907.
17. Laganà, A.; García, E. Mol Phys 1985, 56, 621–627; 1985, 56, 629–639.
18. Martínez, T.; Hernández, M. L.; Alvariño, J. M.; Laganà, A. Aoiz, F. J.; Menéndez, M.; Verdasco, E. Phys Chem Chem Phys 2000, 2, 589–597.
19. Schatz, G. C.; Papaioannou, A.; Pederson, L. A.; Harding, L. B.; Hollebeek, T.; Ho, T. S.; Rabitz, H. J Chem Phys 1997, 107, 2340–2350.
20. Aoiz, F. J.; Bañares, L.; Herrero, V. J. Chem Phys Lett 1999, 310, 277–286.
21. Steckler, R.; Hu, W.-P.; Liu, Y.-P.; Lynch, G. C.; Garrett, B. C.; Isaacson, A. D.; Lu, D.-H.; Melissas, V. S.; Truong, T. N.; Rai, S. N.; Hancock, G. C.; Lauderdale, J.; Joseph, T.; Truhlar, D. G. POLYRATE (Program Version: 6.5); University of Minnesota: Minneapolis, 1995.
22. McRae, G. A.; Cohen, E. A. J Mol Spectrosc 1990, 139, 369–379.
23. Chu, L. T.; Li, Z., in preparation.
24. Levine, R.; Bernstein, R. B. Molecular Reaction Dynamics; 2nd ed.; Oxford University Press: Oxford, 1985.
25. Fukui, K. Acc Chem Res 1981, 14, 363–368.
26. Garrett, B. C.; Redmon, M. J.; Steckler, R.; Truhlar, D.; Baldridge, K. K.; Bartol, D.; Schmidt, M. W.; Gordon, M. S. J Phys Chem 1988, 92, 1476–1488.
27. Peterson, K. A.; Skokov, S.; Bowman, J. B. J Chem Phys 1999, 111, 7446–7456.
28. Alvariño, J. M.; Hernández, M. L.; Laganà, A.; Rodríguez, A. Chem Phys Lett 1999, 313, 299–306.
29. Ha, T. K.; Makarewicz, J. Chem Phys Lett 1999, 299, 637–642.
30. Laganà, A. Computers Chemistry 1980, 4, 137–143.
31. Bittererová, M.; Bowman, J. B.; Peterson, K. A. J Chem Phys, to appear.
32. Balucani, N. Ph.D. Thesis, Università di Perugia, 1993.
33. Drukker, K.; Schatz, G. C. J Chem Phys 1999, 111, 2451–2463.